

# A Customized Self-Assembling Peptide Hydrogel for Dental Pulp Tissue Engineering

Kerstin M. Galler, D.D.S., Ph.D.,<sup>1</sup> Jeffrey D. Hartgerink, Ph.D.,<sup>2</sup> Adriana C. Cavender, B.A.,<sup>3</sup> Gottfried Schmalz, D.D.S., Ph.D.,<sup>1</sup> and Rena N. D'Souza, D.D.S., M.S., Ph.D.<sup>3</sup>

Root canal therapy is common practice in dentistry. During this procedure, the inflamed or necrotic dental pulp is removed and replaced with a synthetic material. However, recent research provides evidence that engineering of dental pulp and dentin is possible by using biologically driven approaches. As tissue engineering strategies hold the promise to soon supersede conventional root canal treatment, there is a need for customized scaffolds for stem cell delivery or recruitment. We hypothesize that the incorporation of dental pulp-derived stem cells with bioactive factors into such a scaffold can promote cell proliferation, differentiation, and angiogenesis. In this study, we used a cell adhesive, enzyme-cleavable hydrogel made from self-assembling peptide nanofibers to encapsulate dental pulp stem cells. The growth factors (GFs) fibroblast growth factor basic, transforming growth factor  $\beta$ 1, and vascular endothelial growth factor were incorporated into the hydrogel via heparin binding. Release profiles were established, and the influence of GFs on cell morphology and proliferation was assessed to confirm their bioactivity after binding and subsequent release. Cell morphology and spreading in three-dimensional cultures were visualized by using cell tracker and histologic stains. Subcutaneous transplantation of the hydrogel within dentin cylinders into immunocompromised mice led to the formation of a vascularized soft connective tissue similar to dental pulp. These data support the use of this novel biomaterial as a highly promising candidate for future treatment concepts in regenerative endodontics.

## Introduction

THE TOOTH IS A SMALL but complex organ comprised of different mineralized matrices that enclose a soft connective tissue termed *dental pulp*. Its manifold functions include providing tooth vitality and sensibility, keeping the dentin moisturized, exerting immune defense, and depositing reparative dentin as a protective mechanism against mechanical stimuli or bacterial noxa. However, dental pulp is vulnerable to caries or trauma. An inflammatory response, if unabated, leads to cell necrosis and inflammation of the periapical tissues. The standard treatment protocol involves root canal therapy, the removal of inflamed or necrotic tissue, and obturation with a synthetic material. Although such therapies have proved fairly effective,<sup>1</sup> the remaining tooth structures are nonvital and brittle due to the loss of the physiologic architecture and function of native dental pulp.

Experimental studies have recently proved that dental pulp stem cells (DPSCs) in combination with a scaffold material are able to generate a soft connective tissue similar to dental pulp<sup>2-7</sup> after subcutaneous transplantation into immunocompromised mice. Currently, the two categories of materials that

are mostly in use for dental pulp tissue engineering are synthetic polymers such as poly(lactic) and poly(glycolic) acid, or natural materials such as type I collagen.<sup>2-7</sup> Both materials have been successfully utilized for specific applications;<sup>8,9</sup> however, neither one combines all the desired characteristics, which can be found in the cells' physiological environment: the extracellular matrix (ECM). The ECM, an intertwined mesh of fibrous proteins and glycosaminoglycans, not only provides anchorage to the cells, but also regulates cellular behavior and communication via structural and chemical signals. Cells bind to and move through the ECM; they degrade, remodel, and rebuild it by synthesizing its components.

Although polymers provide high control over the material properties, are inexpensive, biocompatible, and biodegradable, they fail to mimic the complex physiological functions of the native tissue. Collagen, on the other hand, resembles natural ECM structurally, but is difficult to customize, degrades quickly, and is afflicted with issues of purity and antigenicity. To address these deficiencies, novel synthetic or semisynthetic materials have been developed. Among them, self-assembling peptide nanofibers are a particularly interesting class of biomaterials that offer specific cellular,

<sup>1</sup>Department of Restorative Dentistry and Periodontology, University of Regensburg, Regensburg, Germany.

<sup>2</sup>Departments of Chemistry and Bioengineering, Rice University, Houston, Texas.

<sup>3</sup>Department of Biomedical Sciences, Baylor College of Dentistry, Texas A&M, Dallas, Texas.

biochemical, and biophysical cues. Due to their rational design, ease of synthesis, formation of hydrogels with variable viscoelastic properties, injectability, biocompatibility, biodegradability, and options for the incorporation of bioactive motifs or molecules, they make promising candidate materials for future treatment strategies in regenerative endodontics to support healing and new tissue formation.

#### *Self-assembling multidomain peptides*

Recently, a new type of self-assembling peptide termed “multidomain peptides” (MDPs) was developed in the Hartgerink laboratory.<sup>10</sup> The peptide molecules are designed to display distinct regions of functions called “domains,” which can be changed and optimized independently of one another, thus allowing the design of tailor-made self-assembled materials. The domains are arranged in an ABA block motif that contains an amphiphilic core (the “B” block) surrounded by charged flanking regions (the “A” block). The process of supramolecular assembly (Fig. 1) is driven by the core motif (B) of alternating hydrophilic (serine) and hydrophobic (leucine) amino acid residues. In an aqueous environment, the amino acid side chains segregate to opposing sides of the backbone, and two peptide molecules form a dimer on hydrophobic packing between leucine residues. The B block, thus, drives self-assembly of the peptide molecules into a sandwich-like  $\beta$ -sheet nanofiber in which hydrogen bonding occurs parallel to the growing fiber axis. Charged amino acid residues in the flanking region (A), such as glutamate (negatively charged) or lysine (positively charged), provide water solubility and counteract fiber assembly via electrostatic repulsion. These opposing forces responsible for assembly and repulsion can be balanced to control fiber assembly. Addition of multivalent ions results in elimination of the electrostatic repulsion, followed by physical crosslinking, fiber elongation, entrapment of water, and gelation.

With a fiber diameter of approximately 6 nm, hydrogels created from MDPs mimic the nanoscale dimensions and structure of natural ECM, where cells can bind to the fibers via adhesion molecules, but still interact with other cells.<sup>11</sup> Three-dimensional cell growth within the nanofibrous gels makes these materials promising candidate scaffolds for cell delivery. We recently reported on a variant MDP featuring the cell adhesion motif arginine-glycine-aspartic acid (RGD) as well as an enzyme-cleavable site for cell-mediated degradation.<sup>12</sup> DPSCs in hydrogels resulting from this peptide sequence showed increased viability, spreading, and migration compared with nonbioactive control gels. The objective of this study was to customize this material further by incorporation of growth factors (GFs) relevant to vascularization and DPSC differentiation and to evaluate the potential of this biomaterial for dental pulp tissue engineering.

## **Materials and Methods**

### *Peptide synthesis and gel formation*

The matrix metalloproteinase 2 (MMP-2) sensitive, cell adhesive peptide sequence  $K(SL)_3RG(SL)_3KGRGDS$  was synthesized by solid phase chemistry on an Advanced Chemtech Apex 396 peptide synthesizer by using an optimized protocol.<sup>13</sup> After acylation of the N-termini, peptides

were cleaved from the resin. The crude peptides were dissolved in deionized water at 5 mg/mL and purified by dialysis in semipermeable membranes (molecular weight cut-off 100–500 Da; Spectra/Por, Spectrum Laboratories Inc., Rancho Dominguez, CA) for 5 days. After lyophilization, synthesis of the correct peptide was confirmed by matrix-assisted laser desorption/ionization time-of-flight (Bruker Daltonics, Billerica, MA) mass spectroscopy.

The lyophilized peptides were dissolved at 20 mg/mL in deionized water with 298 mM sucrose, and the pH was adjusted to 7.4. Addition of heparin (heparin sodium salt, Akron Biotech, Boca Raton, FL) at 2 mg/mL in deionized water induced gelation, where the charge of lysine-containing peptides is screened by the negatively charged heparin. Control gels were prepared with 1× phosphate-buffered saline (PBS) instead of heparin solution. The final peptide concentration was 10 mg/mL (1% by weight), the final concentration of heparin 1 mg/mL.

### *Incorporation of GFs and in vitro release kinetics*

Human GFs (Sigma, Saint Louis, MO) were purchased as follows: transforming growth factor  $\beta$ 1 (TGF $\beta$ 1), fibroblast growth factor basic (FGF2), and vascular endothelial growth factor (VEGF). For incorporation into peptide hydrogels, the respective GFs were added to the heparin solution (experimental groups) or PBS (control groups). These solutions were mixed with the peptide stock to trigger gelation. One hundred micro liters of gel were pipetted into wells of a 96-well plate. The concentrations of GF were adjusted to 100 ng for TGF $\beta$ 1 and VEGF, and to 400 ng for FGF2.

Gels were seeded in triplicate, and 200  $\mu$ L of PBS supplemented with 1% bovine serum albumin were added on top. Gels were incubated at 37°C and 5% CO<sub>2</sub> for 14 days. The release media were exchanged at a series of time points (days 1, 2, 3, 5, 7, 10, and 14), where samples were frozen at –80°C until measurement. To verify the binding ability of the nanofiber-heparin complex for the three GFs, the released amounts of TGF $\beta$ 1, FGF2, and VEGF were quantified in all samples by using commercially available enzyme-linked immunosorbent assay (ELISA) kits (R&D TGF $\beta$ 1, FGF2, and VEGF ELISA kits, models DB100B, DFB50, and DVE 00, R&D Systems, Minneapolis, MN).

### *Dental stem cells and cell culture*

Mesenchymal human DPSCs derived from adult third molars.<sup>14</sup> were kindly provided by S. Shi at University of Southern California. Cells were cultured with alpha minimum essential medium supplemented with 10% fetal bovine serum, 50  $\mu$ g/mL L-ascorbic acid 2-phosphate, 100 U/mL penicillin, and 100  $\mu$ g/mL streptomycin, and incubated at 37°C with 5% CO<sub>2</sub>. Cells of passage 5 were used for *in vitro* and *in vivo* experiments.

### *Bioactivity of GFs after release from hydrogels in cell culture*

To demonstrate the effect of GFs on DPSC after release from MDP hydrogels, cell morphology and proliferation rates were assessed in insert cultures. DPSC were seeded into 24-well plates at 2500 cells/well and allowed to adhere for 24 h. For each assay to be performed and for each time point

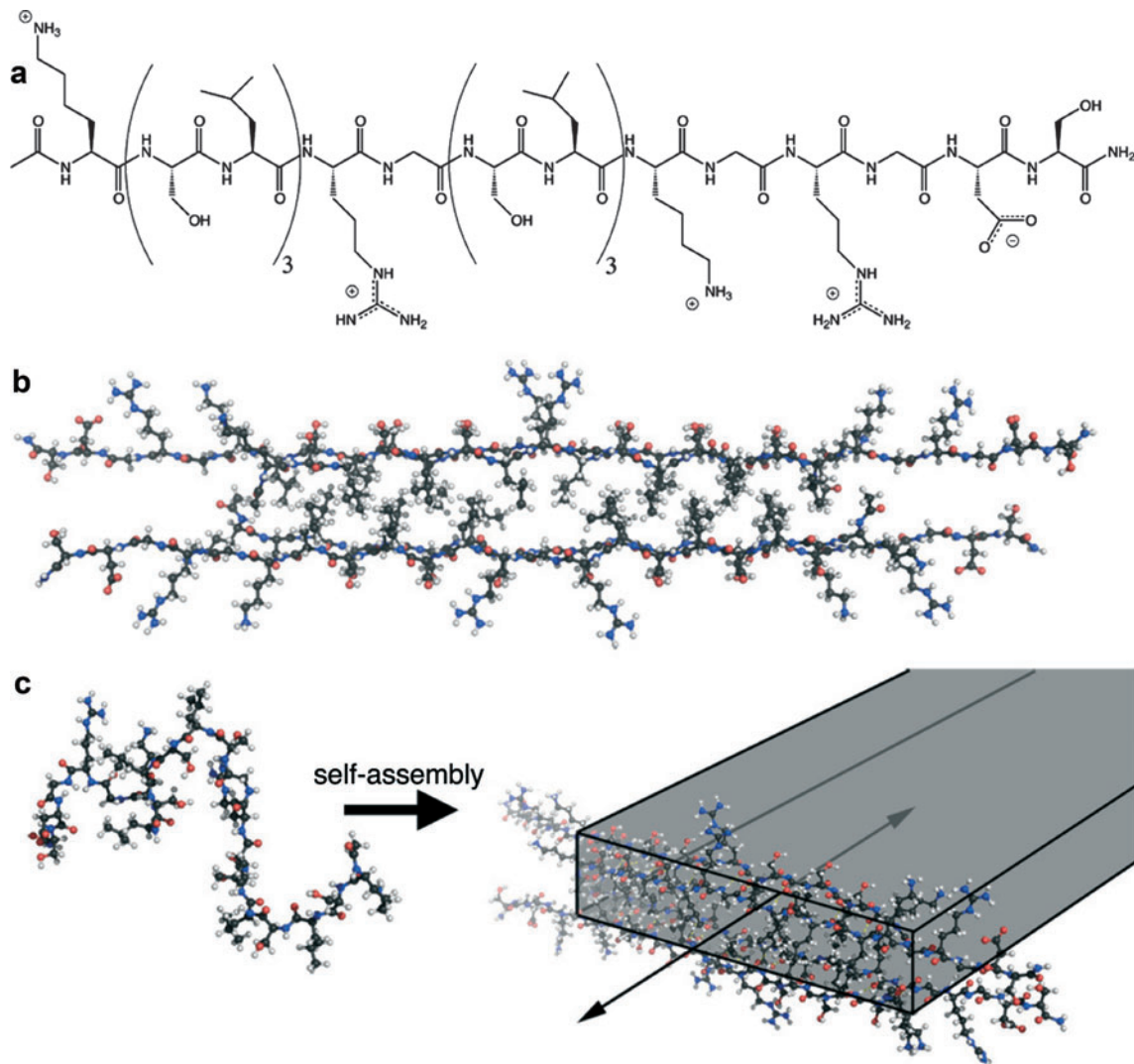


**FIG. 1.** Schematic of peptide and nanofiber structure. **(a)** Chemical structure of the peptide that incorporates alternating hydrophilic/hydrophobic amino acid residues required for self-assembly, an SLRG sequence for enzymatic cleavage, and RGDS sequence for cell adhesion. **(b)** Molecular model showing peptides packing into “hydrophobic sandwiches” that organize the peptides for  $\beta$ -sheet hydrogen bonding. **(c)** Self-assembly of peptides into nanofibers is triggered by addition of oppositely charged multivalent ions such as phosphate or heparin. Color images available online at [www.liebertonline.com/tea](http://www.liebertonline.com/tea)

and culture condition, triplicates were prepared. In control groups, TGF $\beta$ 1 or FGF2 were added to regular cell culture media (as just described) at a concentration of 2.5 and 10 ng/mL, respectively. In experimental groups, heparin- and GF-containing hydrogels were seeded into cell culture inserts. DPSC were grown in a monolayer at the bottom of the well, and the inserts with hydrogels were immersed into the culture medium. Here, a continuous release of GF was to be expected. Twenty-five micro liters of gel were added to each insert, the concentrations of GF amounted to 25 ng for TGF $\beta$ 1 and 100 ng for FGF2. Media in all wells were changed every other day, which led to a replenishment of GF in control groups. Images were taken of DPSC at D3 and D14. To determine cell proliferation, cells were detached from the plates at day 3, 7, and 14 by using trypsin ethylenediaminetetraacetic acid (EDTA), and cell counts were carried out by using a hemocytometer. The results were graphically depicted, and the cell numbers at day 0 were set to 1. Statistical analysis was performed by

using nonparametric Wilcoxon Rank Sum Test to detect differences between the treated groups in comparison to controls at a significance level of  $\alpha=0.05$ .

#### *In vitro cell culture in MDP hydrogels*

DPSC morphology in MDPs was visualized by confocal microscopy. The cells were incubated with 25  $\mu$ M membrane-permeant fluorescein diacetate (Cell Tracker Green CMFDA, Invitrogen, Carlsbad, CA) in cell culture medium for 30 min, resuspended in PBS, and encapsulated in hydrogels at a density of  $1 \times 10^5$  cells per 100  $\mu$ L hydrogel. Addition of PBS (with cells) to the peptide stock solution triggered gelation. Gels were seeded into 96-well plates, and 200  $\mu$ L of cell culture media were added on the top. After incubation for 5 days, samples were fixed in 2% paraformaldehyde and embedded for cryosectioning. Sections of 10  $\mu$ m thickness were prepared on a cryostat microtome, mounted on slides, and stored at  $-20^\circ\text{C}$ . Before

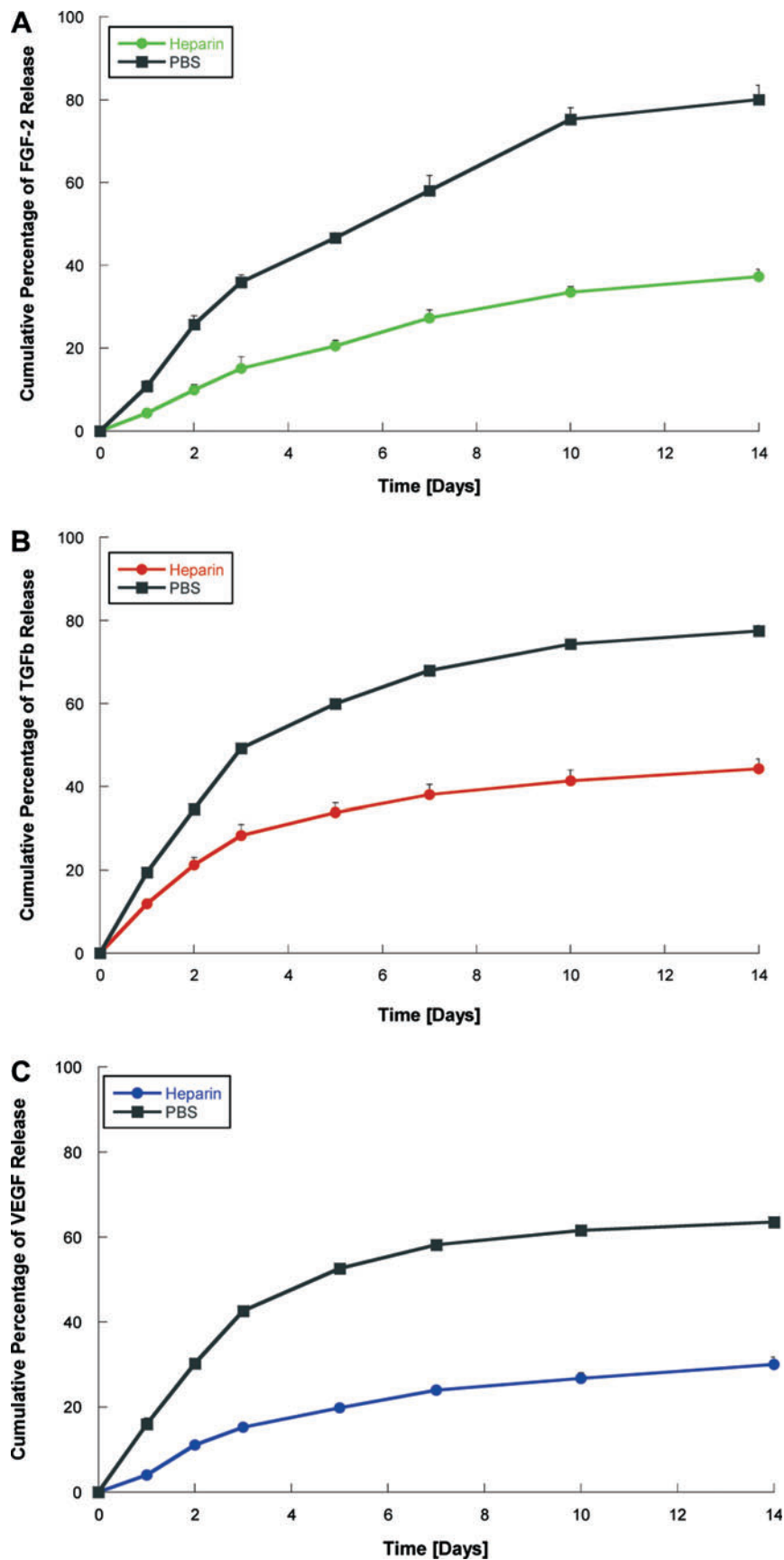
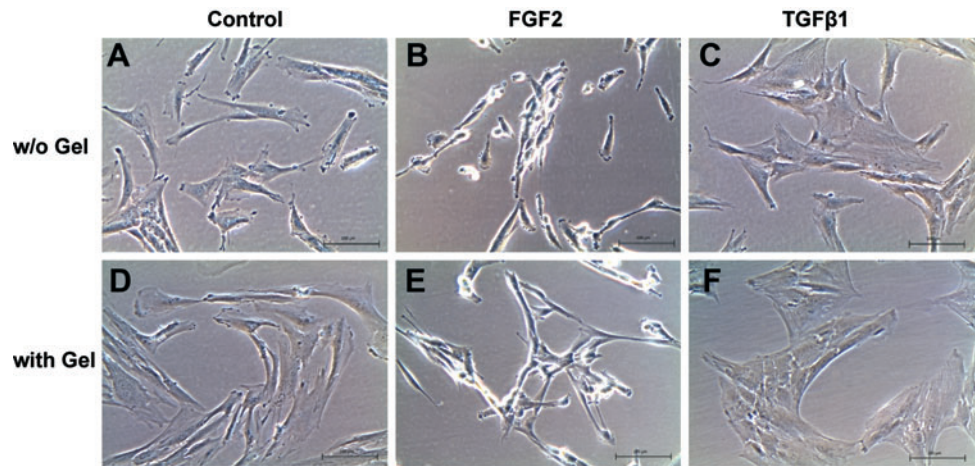


FIG. 2. Growth factor release kinetics. Hydrogels prepared with either PBS (control) or heparin, and growth factors FGF2 (A), TGF $\beta$ 1 (B), or VEGF (C). The amount of growth factor in the supernatant at different time points was determined by ELISA. Graphs show slow release of growth factor from heparin-containing gels. PBS, phosphate-buffered saline; FGF2, fibroblast growth factor basic; TGF $\beta$ 1, transforming growth factor  $\beta$ 1; VEGF, vascular endothelial growth factor; ELISA, enzyme-linked immunosorbent assay. Color images available online at [www.liebertonline.com/tea](http://www.liebertonline.com/tea)

**FIG. 3.** Cell morphology in regular cell culture medium and after addition of growth factors. The upper panel shows DPSC in cell culture medium without supplements (A), and after addition of FGF2 (B), or TGF $\beta$ 1 (C). Culture medium was changed every other day, and growth factors were replenished. Cellular morphology changes from spindle shaped to narrow and elongated with FGF2 or large and flat with TGF $\beta$ 1. The lower panel shows DPSC in presence of MDP hydrogels in inserts, either without growth factors (D), with FGF2 (E), or TGF $\beta$ 1 (F). Analogous changes in morphology can be observed compared with the control panel just described. DPSC, dental pulp stem cell; MDP, multidomain peptide. Color images available online at [www.liebertonline.com/tea](http://www.liebertonline.com/tea)



use, cells were permeabilized with 5% triton X in PBS, and cell nuclei were stained with 4',6-diamidino-2-phenylindole. Cells and hydrogels were visualized by using a Zeiss LSM 510 Meta confocal microscope with an attached photomultiplier tube.

Similarly, untreated DPSC were seeded for histologic analysis. After incubation for 14 days, gels were fixed, embedded in paraffin, sectioned at 6  $\mu$ m thickness, and stained by using a Masson's Trichrome kit.

#### In vivo transplantation

As carriers for MDPs with cells, dentin cylinders were prepared from the coronal parts of extracted human molars.

One cylinder (height: 3 mm; inner diameter: 1 mm; outer diameter: 3 mm) was obtained per root, where the canal was enlarged by using a diamond bur. Samples were stored in 0.5% chloramine at 4°C until further use. Before cell seeding, the dentin cylinders underwent a preparatory procedure carried out in a sterile tissue culture cabinet. They were washed thrice in PBS (1 min each), immersed in 5% sodium hypochlorite for 10 min for disinfection purposes followed by a conditioning step in 17% EDTA for 2 min, with three final washes in PBS.

After cell detachment, cell counts, and centrifugation, cell pellets of  $1 \times 10^7$  cells were resuspended in 100  $\mu$ L peptide stock solution. Gelation was triggered by the addition of

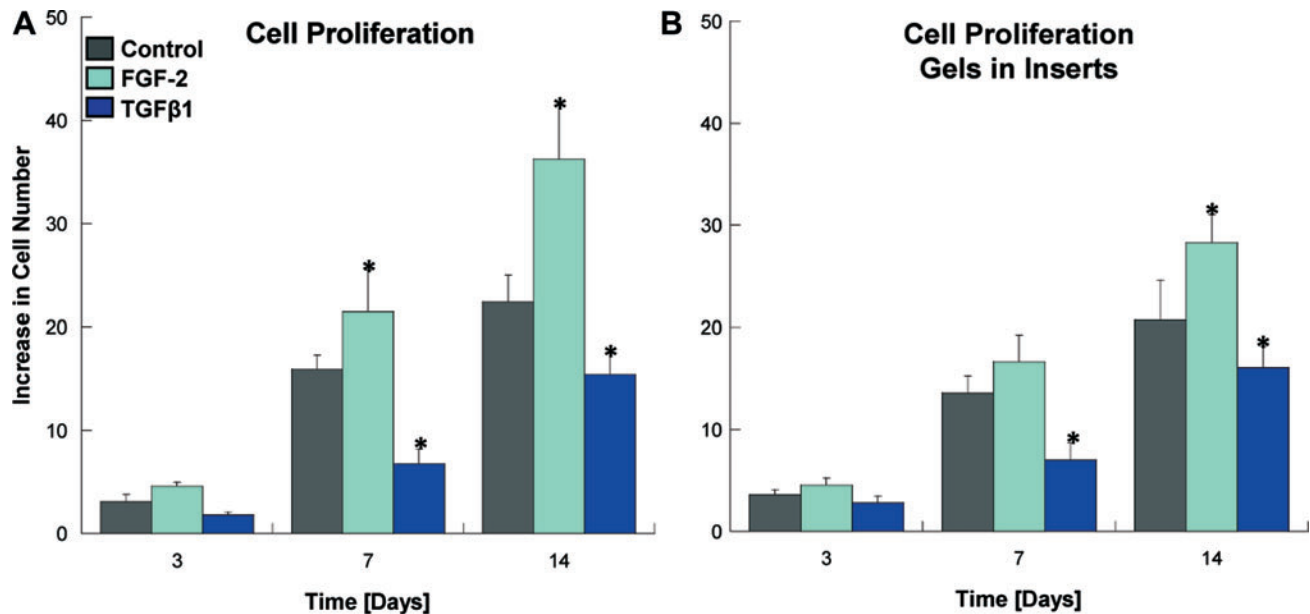


**FIG. 4.** Cell proliferation in regular cell culture medium and after addition of growth factors. The graph shows data from the analogous experiment as described for cell morphology. In monolayer cultures, DPSC proliferation increases after addition of FGF2 and decreases with TGF $\beta$ 1 compared with the control with regular culture medium (A). Similar results can be observed when growth factors are released from heparin-containing hydrogels (B). The cell number at the time point of seeding was set to 1. Depicted are means and standard deviations ( $n=3$ ). Asterisks denote statistical differences in treated groups compared with the control ( $\alpha=0.05$ ). Color images available online at [www.liebertonline.com/tea](http://www.liebertonline.com/tea)

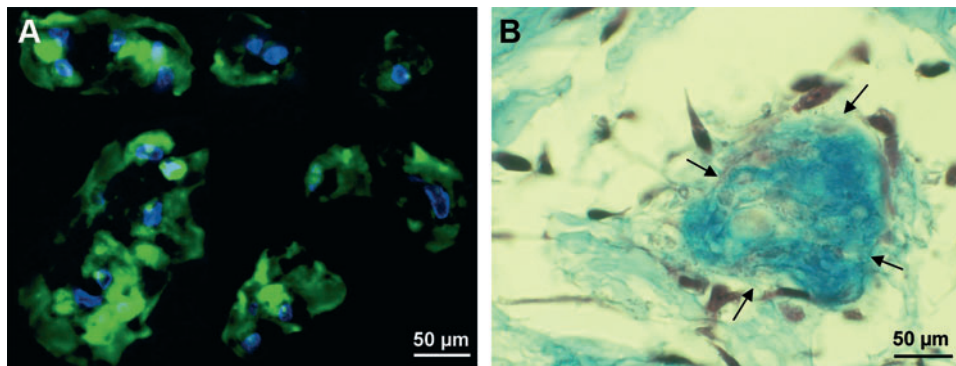


**FIG. 5.** DPSC morphology in three-dimensional hydrogels. Confocal microscopy shows the cells that are stretched out and display cell-cell contacts (A). Histologic Masson's trichrome stain reveals collagen deposition (arrows) near cell clusters (B). Color images available online at [www.liebertonline.com/tea](http://www.liebertonline.com/tea)

heparin solution containing GFs TGFβ1, FGF2, and VEGF (100 ng, 400 ng, and 100 ng/100 μL gel, respectively) in experimental groups. Twenty micro liters of hydrogel were seeded into each cylinder containing  $2 \times 10^6$  cells. Cylinders with GF-free gels or cell-free gels served as controls. The groups are defined as follows:

- (A) MDP, no GF, no cells (baseline control)
- (B) MDP, GF, no cells (cell-free control)
- (C) MDP, no GF, DPSC (GF-free control)
- (D) MDP, GF, DPSC

These constructs were implanted into the backs of immunocompromised mice (8- to 10-week-old females, strain CrI: NIH-*Lyst*<sup>bgFoxn1<sup>nu</sup>Btk<sup>kid</sup></sup> or NIH III; Charles River, Wilmington, MA) according to the specifications of an approved small animal protocol. Four implants were placed per animal, 10 implants per group. After sacrifice 5 weeks later, the implants were removed and fixed in 2% paraformaldehyde for 24 h. Dentin cylinders were demineralized in Morse's solution for 2 weeks. The constructs were then embedded in paraffin, sectioned, and prepared for histology and immunohistochemistry.

Sections were stained with hematoxylin and eosin (H&E) and Masson's trichrome for collagen deposition. For dentin sialoprotein (Dsp), a 1:100 dilution of anti-human Dsp antibody was applied (Santa Cruz Biotechnology, Santa Cruz, CA). For detection of endothelial cells and, thus, microvascular networks, a 1:100 dilution of anti-human Factor VIII antibody was used (Lab Vision, Fremont, CA). Color development was performed with Dako EnVision + system kit (AEC, Dakocytomation, Hamburg, Germany), and sections were counterstained with hematoxylin. For controls, one section per group was treated with PBS instead of primary antibody.

## Results

### *Incorporation of GFs and in vitro release kinetics*

The incorporation of heparin was successful at a concentration of 1 mg/mL, where positively charged lysine binds the highly negatively charged heparin to induce gelation. The release profiles of VEGF, TGFβ1, and FGF2 in heparin-containing and PBS-containing (control) gels are depicted in Figure 2, which presents the time course of total cumulative release of the GF. Although in control gels, 60%–80% of GF were released after 10 days, the presence of heparin caused a delayed release, which confirms the ability of heparin-binding nanostructures to bind the three GFs and slow their release.

### *Cell culture with GF release from hydrogels*

Cell morphology of DPSC is depicted in Figure 3. The control experiment shows different cell morphology and proliferation rates when DPSC are treated with TGFβ1 or FGF2. In regular cell culture media, the cells show their typical spindle-shaped, fibroblast-like morphology. With FGF2, the cells appear much more elongated and cover a smaller area on the tissue culture plate. TGFβ1 induced the opposite effect, where the cells appear larger and flatter. Cell proliferation (Fig. 4) was increased after treatment with FGF2, but decreased with TGFβ1. In the experimental groups, where GF-containing hydrogels were placed in inserts and immersed in the cell culture medium, which nourishes the cells that grow in a monolayer underneath, the effects on morphology and proliferation were similar. Statistically significant differences are observed when compared with the untreated cells after day 3. This confirms that the GFs bound to and consecutively released from the hydrogels exert bioactivity and show the expected effect on cellular behavior.

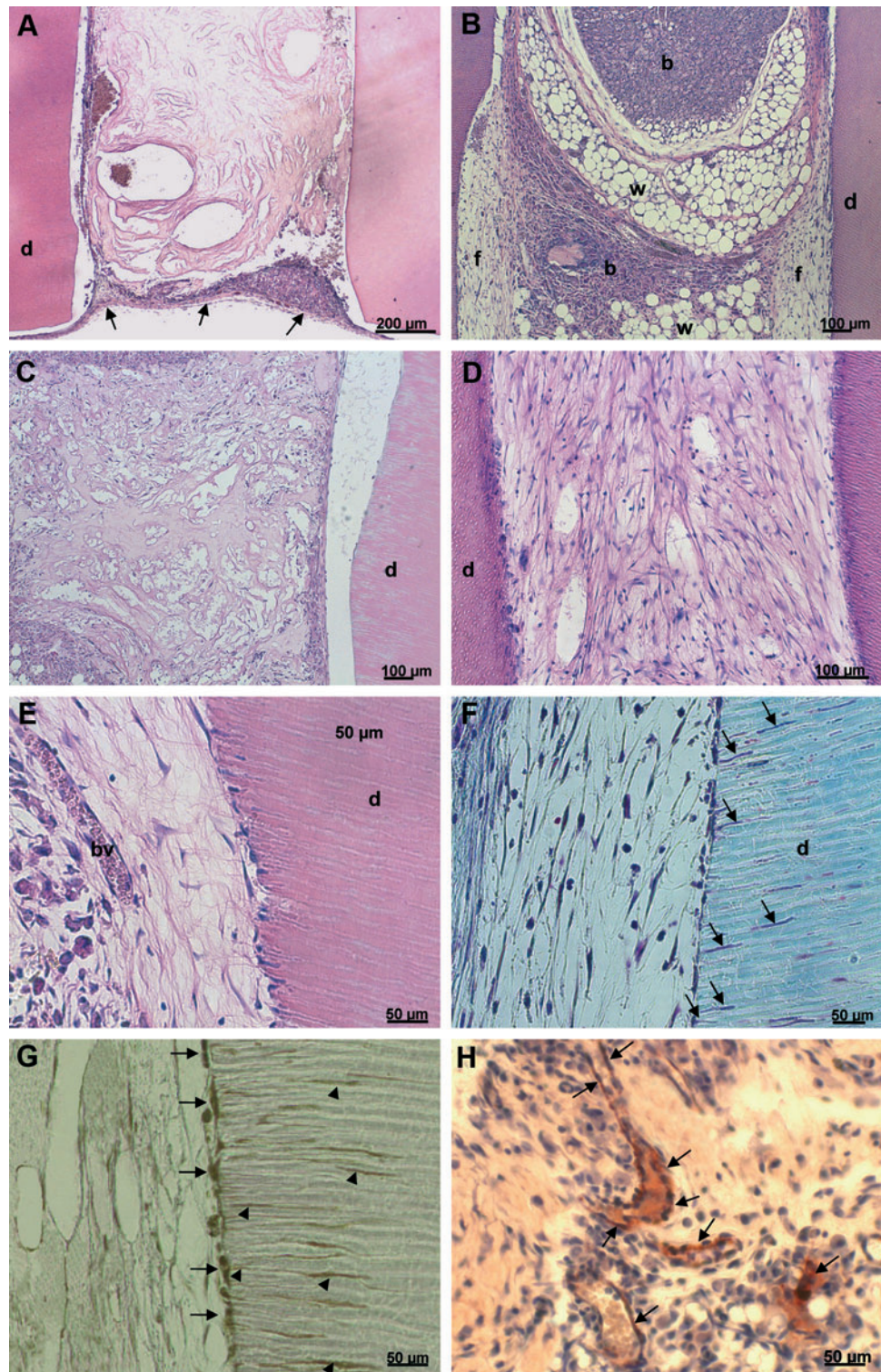
### *Cell morphology in GF-laden hydrogels*

Figure 5 displays cell morphology of DPSC in the three-dimensional environment after seeding into peptide hydrogels. The cells appear elongated and stretched out, they are in contact with neighboring cells. Histology shows further that cell clusters in the hydrogel produce collagen as their own ECM to replace the synthetic carrier.

### *In vivo experiments*

Histologic analysis of the constructs after 5 weeks *in situ* are shown in Figure 6. In dentin cylinders without cells and GFs, only the MDP matrix is visible, and the cylinder is enclosed in a fibrous capsule (Fig. 6A). However, the presence of GFs attracts host cells into the cylinders, which is filled with a mixture of tissues, including brown and white fatty tissue as well as soft connective fibrous tissue (Fig. 6B). After the seeding of DPSC in the hydrogels without GFs, the cells do not proliferate enough to fill the cylinder and fully degrade the synthetic matrix; thus, the formation of a tissue cannot be observed (Fig. 6C). DPSC in hydrogels with GFs form a vascularized soft connective tissue resembling dental pulp (Fig. 6D–H). The cells degrade the hydrogel and replace it with a collagenous ECM (Fig. 6E, F). Cells at the cell-dentin interface appear flat and in intimate association with the dentin wall, where cellular processes extend into the dentinal tubules (Fig. 6F). These cells express the dentin-specific

**FIG. 6.** Histologic analysis of constructs after subcutaneous transplantation. Dentin cylinders of group A are filled with only the hydrogel remnants and enclosed by a fibrous capsule (arrows) (A). In group B, the growth factors present in cell-free gels attract host cells from various tissues: brown adipose tissue (b), white adipose tissue with vacuoles (w), and fibrous tissue (f) (B). Group C displays DPSC embedded in the gel matrix (C). In group D, DPSC have formed a pulp-like soft connective tissue (D). Higher magnification shows blood vessels (bv) and a cell layer in intimate association with the dentin wall (E). The cells extend processes into the dentinal tubules (arrows), a characteristic of odontoblast cell morphology (F). The cell layer adjacent to the dentin as well as the cellular processes stain positive for dentin sialoprotein (G). Microvessels can be visualized after immunohistochemistry with Factor VIII-antibody (H). A–E: Hematoxylin and eosin. F: Masson's trichrome. G, H: Immunohistochemistry. d: dentin. Color images available online at [www.liebertonline.com/tea](http://www.liebertonline.com/tea)



marker (Dsp; Fig. 6G). Microvessels are present, which is visible after H&E stain (Fig. 6E) as well as after immunohistochemistry for endothelial Factor VIII (Fig. 6H).

## Discussion

In this study, we describe a novel dental pulp engineering approach, in which all aspects of the classical tissue engi-

neering triad are controlled and tailored to create optimized conditions for regeneration. These methods are highly translational for clinical applications and involve the use of a suitable cell line, the rational design of a custom-made material, and the selection of inductive GFs relevant for cell proliferation and odontogenic differentiation.

The cells that appear most applicable for this approach are DPSCs. During the past decade, mesenchymal stem cells

have been isolated from a variety of tooth-derived tissues, including dental pulp of deciduous<sup>15</sup> as well as permanent teeth,<sup>14</sup> periodontal ligament,<sup>16</sup> dental follicle,<sup>17</sup> or apical papilla.<sup>18</sup> The properties of these different cell populations have been characterized by various groups.<sup>19</sup> Although they all possess stem cell properties, distinct differences exist regarding their proliferation rates, stemness, gene expression profiles, and differentiation potential.<sup>19,20</sup> The cell types derived from dental pulp and apical papilla are capable of dentin formation; however, stem cells from deciduous teeth do not generate complex structures composed of both dentin and dental pulp, which can be observed for DPSC and apical papilla cells. This feature makes the latter most applicable for dentin-pulp complex engineering.

The self-assembling peptide matrix developed in this study provides several advantages, which make it superior to conventional, non-custom-made materials. Structurally, the peptide nanofibers are a true mimic of ECM due to their nanoscale dimensions. The small fiber diameter allows cells to bind to the cell-adhesive RGD motif, but still form contacts and interact with other cells in all three dimensions.<sup>11</sup> Our recent work demonstrated increased proliferation rates of DPSCs in peptide gels containing the RGD motif,<sup>12</sup> where cell adhesion can be regarded as a prerequisite of proliferation. Further, the peptide sequence used in this study features an enzyme-cleavable site for cell-mediated degradation. The cleavage motif was designed to be susceptible to MMP-2, an MMP expressed by fibroblasts and odontoblasts in healthy dental pulps to remodel their environment.<sup>21</sup> The compatibility with DPSCs has been recently described,<sup>12</sup> and data presented here show DPSC spreading and formation of a collagenous matrix in the peptide hydrogel. In terms of future clinical applications, viscoelastic properties and shear-recovery are of importance. MDP crosslinking and stiffness are tunable by sequence modification.<sup>13</sup> The hydrogel chosen for this study features viscoelastic properties adjusted to a clinical procedure where the material can be injected into the root canal using a syringe, but recovers to the original stiffness *in situ*.<sup>13</sup>

The GFs that were incorporated into the peptide hydrogel were chosen to promote both angiogenesis and DPSC differentiation. Although angiogenesis is of importance for most tissue engineering approaches to ensure adequate supply of nutrients, it is of special concern for pulp engineering as we are trying to vascularize a long and narrow cylinder, the root canal, with only one opening at the root apex. Among a variety of angiogenic GFs, which induce capillary networks to sprout from pre-existing ones, VEGF has been identified as a pivotal stimulator of endothelial cell migration and proliferation.<sup>22</sup> Proof of principle exists for the incorporation of VEGF into different hydrogel scaffolds via heparin binding and effectiveness of these systems *in vivo*.<sup>23,24</sup> TGF $\beta$ 1 has long been recognized as a modulator of dental pulp cell proliferation, differentiation, and the upregulation of ECM synthesis.<sup>25</sup> FGF2 is able to induce cell migration and proliferation in dental pulp cells without affecting their differentiation abilities.<sup>26</sup> The combination of these two GFs seems to evoke synergistic effects and stimulate proliferation as well as cytodifferentiation and mineralization.<sup>27</sup> Our study demonstrates incorporation of these three GFs in the synthetic peptide matrix, the

release profiles show delayed liberation from heparin-containing gels, and the bioactivity of TGF $\beta$ 1 and FGF2 is proved in cell culture. We have a custom-made, bioactive ECM mimic at hand that is able to support the formation of a vascularized soft connective tissue similar to dental pulp after transplantation *in vivo*. The GFs by themselves were able to attract host cells into the cylinders, which is in accordance with a recent report where host cells migrated into human tooth roots laden with chemotactic factors after implantation in the dorsum of rats.<sup>28</sup> Further, they supported cell proliferation and differentiation when seeded with DPSC.

From a clinical point of view, the hydrogels are ideally suited for injection into the root canal. It is imaginable to combine this scaffold with autologous stem cells, for example, from disposable sources such as surgically removed wisdom teeth. Another application could be a cell-free material, possibly with an extended array of GFs and chemoattractants, which is able to activate resident stem cells from remaining pulp tissue or the periapical region and to induce migration into the root canal, cytodifferentiation, and new dentin formation. Additionally, GFs embedded in the dentin matrix and released by conditioning with chelators or acids<sup>29</sup> before the insertion of cells and matrix could optimize this approach. Such therapies hold promise for regenerative endodontics that aims at preserving the integrity of both the soft and hard tissues of the tooth. Success in developing such approaches are likely to lead to applications for other systems, such as periodontal tissue regeneration.

#### Disclosure Statement

No competing financial interests exist.

#### References

1. Sjogren, U., Hagglund, B., Sundqvist, G., and Wing, K. Factors affecting the long-term results of endodontic treatment. *J Endod* **19**, 498, 1990.
2. Cordeiro, M.M., Dong, Z., Kaneko, T., Zhang, Z., Miyazawa, M., Shi, S., Smith, A.J., and Nör J.E. Dental pulp tissue engineering with stem cells from exfoliated deciduous teeth. *J Endod* **34**, 962, 2008.
3. Sakai, V.T., Zhang, Z., Dong, Z., Neiva, K.G., Machado, M.A., Shi, S., Santos, C.F., and Nör, J.E. SHED differentiate into functional odontoblasts and endothelium. *J Dent Res* **89**, 791, 2010.
4. Huang, G.T., Yamaza, T., Shea, L.D., Djouad, F., Kuhn, N.Z., Tuan, R.S., and Shi, S. Stem/Progenitor cell-mediated *de novo* regeneration of dental pulp with newly deposited continuous layer of dentin in an *in vivo* model. *Tissue Eng Part A* **16**, 605, 2010.
5. Nakashima, M., and Iohara, K. Regeneration of dental pulp by stem cells. *Adv Dent Res* **23**, 313, 2011.
6. Iohara, K., Zheng, L., Ito, M., Ishizaka, R., Nakamura, H., Ito, T., Matsushita, K., and Nakashima, M. Regeneration of dental pulp after pulpotomy by transplantation of CD31(-)/CD146(-) side population cells from a canine tooth. *Regen Med* **4**, 377, 2009.
7. Prescott, R.S., Alsanea, R., Fayad, M.I., Johnson, B.R., Wenckus, C.S., and Hao, J. *In vivo* generation of dental pulp-like tissue by using dental pulp stem cells, a collagen



- scaffold, and dentin matrix protein 1 after subcutaneous transplantation in mice. *J Endod* **34**, 421, 2008.
8. Van Blitterswijk, C., ed. *Tissue Engineering*. London, United Kingdom: Elsevier, 2008.
  9. Glowacki, J., and Mizuno, S. Collagen scaffolds for tissue engineering. *Biopolymers* **89**, 338, 2008.
  10. Dong, H., Paramonov, S.E., Aulisa, L., Bakota, E.L., and Hartgerink, J.D. Self-assembly of multidomain peptides: balancing molecular frustration controls conformation and nanostructure. *J Am Chem Soc* **129**, 12468, 2007.
  11. Segers, V.F., and Lee, R.T. Local delivery of proteins and the use of self-assembling peptides. *Drug Discov Today* **12**, 56, 2007.
  12. Galler, K.M., Aulisa, L., Regan, K.R., D'Souza, R.N., and Hartgerink, J.D. Self-assembling multidomain peptide hydrogels: designed susceptibility to enzymatic cleavage allows enhanced cell migration and spreading. *J Am Chem Soc* **132**, 3217, 2010.
  13. Aulisa, L., Dong, H., and Hartgerink, J.D. Self-assembly of multidomain peptides: sequence variation allows control over cross-linking and viscoelasticity. *Biomacromolecules* **10**, 2694, 2009.
  14. Gronthos, S., Mankani, M., Brahimi, J., Robey, P.G., and Shi, S. Postnatal human dental pulp stem cells (DPSCs) *in vitro* and *in vivo*. *Proc Natl Acad Sci U S A* **97**, 13625, 2000.
  15. Miura, M., Gronthos, S., Zhao, M., Lu, B., Fisher, L.W., Robey, P.G., and Shi, S. SHED: stem cells from human exfoliated deciduous teeth. *Proc Natl Acad Sci U S A* **100**, 5807, 2003.
  16. Seo, B.M., Miura, M., Gronthos, S., Bartold, P.M., Batouli, S., Brahimi, J., Young, M., Robey, P.G., Wang, C.Y., and Shi, S. Investigation of multipotent postnatal stem cells from human periodontal ligament. *Lancet* **364**, 149, 2004.
  17. Morszeck, C., Götz, W., Schierholz, J., Zeilhofer, F., Kühn, U., Möhl, C., Sippel, C., and Hoffmann, K.H. Isolation of precursor cells (PCs) from human dental follicle of wisdom teeth. *Matrix Biol* **24**, 155, 2005.
  18. Sonoyama, W., Liu, Y., Yamaza, T., Tuan, R.S., Wang, S., Shi, S., and Huang, G.T. Characterization of the apical papilla and its residing stem cells from human immature permanent teeth: a pilot study. *J Endod* **34**, 166, 2008.
  19. Huang, G.T., Gronthos, S., and Shi, S. Mesenchymal stem cells derived from dental tissues vs. those from other sources: their biology and role in regenerative medicine. *J Dent Res* **88**, 792, 2009.
  20. Shi, S., Bartold, P.M., Miura, M., Seo, B.M., Robey, P.G., and Gronthos, S. The efficacy of mesenchymal stem cells to regenerate and repair dental structures. *Orthod Craniofac Res* **8**, 191, 2005.
  21. Gusman, H., Santana, R.B., and Zehnder, M. Matrix metalloproteinase levels and gelatinolytic activity in clinically healthy and inflamed human dental pulps. *Eur J Oral Sci* **110**, 353, 2002.
  22. Ferrara, N. Role of vascular endothelial growth factor in physiologic and pathologic angiogenesis: therapeutic implications. *Semin Oncol* **29**, 10, 2002.
  23. Pike, D.B., Cai, S., Pomraning, K.R., Firpo, M.A., Fisher, R.J., Shu, X.Z., Prestwich, G.D., and Peattie, R.A. Heparin-regulated release of growth factors *in vitro* and angiogenic response *in vivo* to implanted hyaluronan hydrogels containing VEGF and bFGF. *Biomaterials* **27**, 5242, 2006.
  24. Rajangam, K., Behanna, H.A., Hui, M.J., Han, X., Hulvat, J.F., Lomasney, J.W., and Stupp, S.I. Heparin binding nanostructures to promote growth of blood vessels. *Nano Lett* **6**, 2086, 2006.
  25. Melin, M., Joffre-Romeas, A., Farges, J.C., Couble, M.L., Magloire, H., and Bleicher, F. Effects of TGFbeta1 on dental pulp cells in cultured human tooth slices. *J Dent Res* **79**, 1689, 2000.
  26. Shimabukuro, Y., Ueda, M., Ozasa, M., Anzai, J., Takedachi, M., Yanagita, M., Ito, M., Hashikawa, T., Yamada, S., and Murakami, S. Fibroblast growth factor-2 regulates the cell function of human dental pulp cells. *J Endod* **35**, 1529, 2009.
  27. He, H., Yu, J., Liu, Y., Lu, S., Liu, H., Shi, J., and Jin, Y. Effects of FGF2 and TGFbeta1 on the differentiation of human dental pulp stem cells *in vitro*. *Cell Biol Int* **32**, 827, 2008.
  28. Suzuki, T., Lee, C.H., Chen, M., Zhao, W., Fu, S.Y., Qi, J.J., Chotkowski, G., Eisig, S.B., Wong, A., and Mao, J.J. Induced migration of dental pulp stem cells for *in vivo* pulp regeneration. *J Dent Res* **90**, 1013, 2011.
  29. Zhao, S., Sloan, A.J., Murray, P.E., Lumley, P.J., and Smith, A.J. Ultrastructural localisation of TGF-beta exposure in dentine by chemical treatment. *Histochem J* **32**, 489, 2000.

Address correspondence to:

Kerstin M. Galler, D.D.S., Ph.D.

Department of Restorative Dentistry and Periodontology

University of Regensburg

Franz-Josef-Strauss-Allee 11

Regensburg 93053

Germany

E-mail: kerstin.galler@klinik.uni-regensburg.de

Rena N. D'Souza, D.D.S., M.S., Ph.D.

Department of Biomedical Sciences

Baylor College of Dentistry

3302 Gaston Ave.

Dallas, TX 75246

E-mail: rdsouza@bcd.tamhsc.edu

Received: April 20, 2011

Accepted: August 8, 2011

Online Publication Date: September 27, 2011